Supplementary Material (ESI) for CrystEngComm


# Mechanosensitive metal–ligand bonds in the design of new coordination compounds

**Krunoslav Užarević,* Mirta Rubčić,* Maja Radić, Andreas Puškarić and Marina Cindrić**

*Department of Chemistry, Faculty of Science, University of Zagreb, Horvatovac 102a, 10000 Zagreb, Croatia. E-mail: kruno@chem.pmf.hr; mirta@chem.pmf.hr.*

**Materials.** Acetylacetone, 3-methoxysalicylaldehyde, 2-amino-3-hydroxypyridine, and $(NH_4)_6Mo_7O_{24}\cdot 4H_2O$ were obtained from Sigma-Aldrich and used without further purification. $[MoO_2(C_5H_7O_2)_2]$, *cis*-dioxo*bis*(2,4-pentanedionato)molybdenum(VI), was prepared according to the literature methods.[i] Solvents and concentrated acids (p.a. grade) were purchased from Kemika, Zagreb.

**Methods.** Elemental analyses were performed by Central Analytical Service, "Ruđer Bošković" Institute, Zagreb. IR spectra were recorded on PerkinElmer *Spectrum RXI* FT-IR spectrometer (KBr pellet technique, 4000–400 $cm^{-1}$ range, 2 $cm^{-1}$ step). Temperature-resolved IR was collected on Bruker VECTOR 22 FT-IR spectrometer (KBr pellet technique, 4000–400 $cm^{-1}$ range, 2 $cm^{-1}$ step) in the range from 25 to 180 °C. Thermogravimetric analyses (TGA) were performed on a Mettler-Toledo TGA/SDTA851[e] thermobalance using aluminum crucibles under nitrogen or oxygen stream with the heating rate of 5 °C $min^{-1}$. In all experiments the temperature ranged from 25 to 600 °C. The results were processed with the Mettler STARe 9.01 software. DSC measurements were performed on the Mettler–Toledo DSC823[e] calorimeter with STARe SW 9.01 in the range from 25 to maximally 600 °C (5 °C$min^{-1}$) under the nitrogen stream.

## Synthetic procedures

**Synthesis of *N*-3-methoxysalicylidene-2-amino-3-hydroxypyridine, $H_2L$.** Equimolar amounts (0.82 mmol) of 2-amino-3-hydroxypyridine and 2-hydroxy-3-methoxybenzaldehyde were added in 5 mL of methanol and refluxed for 1.5 h. Dark red crystalline product was isolated after two days standing at room temperature. Yield: 51%. Elemental analysis (Calc. (Found) for $C_{13}H_{12}N_2O_3$): C 63.93 (63.97); H 4.95 (4.88); N 11.47 (11.40). IR (KBr, $cm^{-1}$): 3428 br ($\nu_{O-H}$); 3050, 3006 br ($\nu_{C-H}$); 1617, 1577, 1544, 1520 ($\nu_{C=O}$ and $\nu_{C=N}$).

**Syntheses of alcohol complexes, $[MoO_2L(ROH)]$.**

**Synthesis of $[MoO_2L(MeOH)]$ (I(Me))**

**Method AM. Solution synthesis by the reaction of $[MoO_2(acac)_2]$ and $H_2L$.** $[MoO_2(acac)_2]$ (94 mg; 0.29 mmol) was added to a methanolic solution (5 mL) of $H_2L$ (70 mg; 0.29 mmol) and refluxed for 1.5 h. After 3 days standing at the room temperature, yellow crystals were filtered off and dried. Yield: 77 %. Elemental analysis ((Calc. (Found) for $C_{14}H_{14}N_2O_6Mo$): C 41.81 (41.92); H 3.51 (3.50); N 6.96 (7.05)). IR (KBr, $cm^{-1}$): 3469 br ($\nu_{O-H}$); 2928( $\nu_{C-H}$);

2562 ($\nu_{O-H\cdots N}$); 1605, 1584, 1553 ($\nu_{C=O}$ and $\nu_{C=N}$); 1014 ($\nu_{C-O,}$ methanol); 938, 914 ($\nu_{Mo=O}$, terminal).

**Method BM. Sorption of methanol vapours.** $[MoO_2L]$ or $[MoO2L]_n$ (0.04 mmol) were placed in the sealed beaker with methanol vapours. Orange or brown precursor changed colour after 10 minutes standing at RT. Analyses (elemental analysis, PXRD, IR) of the product show that the synthesised yellow crystals are $[MoO_2L(MeOH)]$. Yield: 100%.

**Synthesis of $[MoO_2L(EtOH)]$ (I(Et))**

**Method AE. Solution synthesis by the reaction of $[MoO_2(acac)_2]$ and $H_2L$.** $[MoO_2(acac)_2]$ (94 mg; 0.29 mmol) was added to an ethanolic solution (5 mL) of $H_2L$ (70 mg; 0.29 mmol) and refluxed for 1.5 h. After 1 day standing at the room temperature, orange crystals were filtered off and dried. Yield: 66 %. Elemental analysis ((Calc. (Found) for $C_{15}H_{16}N_2O_6Mo$): C 43.28 (43.20); H 3.87 (3.74); N 6.73 (6.90)). IR (KBr, $cm^{-1}$): 3447 br ($\nu_{O-H}$); 2821 ( $\nu_{C-H}$); 1605, 1581, 1553 ($\nu_{C=O}$ and $\nu_{C=N}$); 1035 ($\nu_{C-O,}$ ethanol); 933, 911 ($\nu_{Mo=O}$, terminal).

**Method BE. Sorption of ethanol vapours.** $[MoO_2L]$ or $[MoO2L]_n$ (0.04 mmol) were placed in the sealed beaker and in ethanol vapours. Orange ($[MoO_2L]$) or brown precursor ($[MoO2L]_n$) changed colour after 1 day standing at RT. Analyses (elemental analysis, PXRD, IR) of the product show that the synthesised orange powder is $[MoO_2L(EtOH)]$ (**I(Et)**). Yield: 100%.

**Synthesis of $[MoO_2L(PrOH)]$ (I(Pr))**

**Method AP. Solution synthesis by the reaction of $[MoO_2(acac)_2]$ and $H_2L$.** $[MoO_2(acac)_2]$ (94 mg; 0.29 mmol) was added to an ethanolic solution (5 mL) of $H_2L$ (70 mg; 0.29 mmol) and refluxed for 1.5 h. Orange-red crystals were filtered off and dried after 1 day standing at the room temperature. Yield: 89 %. Elemental analysis ((Calc. (Found) for $C_{16}H_{18}N_2O_6Mo$): C 44.66 (44.71); H 4.22 (4.17); N 6.51 (6.50)). IR (KBr, $cm^{-1}$): 3419 br ($\nu_{O-H}$); 2957, 2835 ( $\nu_{C-H}$); 1598, 1581, 1553 ($\nu_{C=O}$ and $\nu_{C=N}$); 1039 ($\nu_{C-O,}$ propanol); 936, 913 ($\nu_{Mo=O}$, terminal).

**Method BP. Sorption of propanol vapours.** $[MoO_2L]$ or $[MoO_2L]_n$ (0.04 mmol) were placed in the sealed beaker with propanol vapours. Precursors changed colour after 2 days standing at RT. Analyses (elemental analysis, PXRD, IR) of the product denoted the synthesised red powder as $[MoO_2L(PrOH)]$ (**I(Pr)**). Yield: 100%.

**Synthesis of $[MoO_2(L)]$ (I).** Alcohol complexes ($[MoO_2L(ROH)]$, ROH = MeOH, EtOH, PrOH) were ground using a mortar and a pestle for 5 minutes. Depending on the complex ground, different time of grinding was needed for yellow powders to change colour to dark orange (5 minutes for $[MoO_2L(MeOH)]$; 15 minutes for $[MoO_2L(EtOH)]$ and 35 minutes for $[MoO_2L(PrOH)]$). The process was repeated under inert atmosphere (argon) with the same result. Amorphous (PXRD) substance thus prepared, $[MoO_2(L)]$, was collected and analyzed. Elemental analysis ((Calc. (Found) for $C_{13}H_{10}N_2O_5Mo$): C 42.18 (42.02); H 2.72 (2.56); N 7.57 (7.63). IR (KBr, $cm^{-1}$): 2936, 2836 ($\nu_{C-H}$) 1598, 1553 ($\nu_{C=O}$ and $\nu_{C=N}$); 939, 911 ($\nu_{Mo=O}$, terminal).

**Synthesis of $[MoO_2(L)]_n$ ($(I)_n$)**

**Method I. Heating of alcohol complexes ($[MoO_2L(ROH)]$, ROH = MeOH, EtOH, PrOH).** Synthesis of $[MoO_2(L)]_n$ (**$(I)_n$**) was conducted using simple furnace or thermogravimetric balance. Alcohol complexes were placed in a crucible and heated to 210 °C, at 5 °C/min. In all cases this procedure resulted with a brown product, $[MoO_2(L)]_n$ (**$(I)_n$**) in quantitative yield. Elemental analysis ((Calc. (Found) for $C_{13}H_{10}N_2O_5Mo$): C 42.18 (42.06); H 2.72 (2.80); N 7.57 (7.55). IR (KBr, $cm^{-1}$): 2925, 2834 ($\nu_{C-H}$); 1606, 1594, 1551 ($\nu_{C=O}$ and $\nu_{C=N}$); 941 ($\nu_{Mo=O}$, terminal); 814 s, br ($\nu_{Mo=O\cdots Mo}$).

**Method II.** $[MoO_2(L)]$ (**I**) was heated from 25 °C to 130 °C (5 °C $min^{-1}$) and cooled to room temperature. Analytical and spectral data for the isolated product obtained by this method are in agreement with those of the compound prepared according to the method I.

**Synthesis of $[MoO_2L(im)]$ (I(Im)) and $[MoO_2L(im)]\cdot CH_3CN$ (I(Im)·$CH_3CN$)**

**Solution synthesis from dichloromethane or acetonitrile.** $[MoO_2L]_n$ (**$(I)_n$**) (15 mg; 0.04 mmol) was diluted in 1.5 mL of heated dry dichloromethane. To such prepared solution equimolar amount of imidazole was added. Orange-red needle-like crystals were filtered off and dried after 2 days standing at the room temperature. Yield: 52%. When the solvent used were acetonitrile, red prisms were obtained. Analyses (elemental analysis, PXRD, IR) showed that the synthesised product is $[MoO_2L(im)]\cdot CH_3CN$ solvate. Product is stable at the air, even when heated to 40 °C. Yield: 46%. Elemental analysis for **$[MoO_2L(im)]$** ((Calc. (Found) for $C_{16}H_{14}N_4O_5Mo$): C 43.85 (43.76); H 3.22 (3.16); N 12.78 (12.64)). IR (KBr, $cm^{-1}$): 3284m ($\nu_{N-H,\ imidazole}$); 2944, 2837 ($\nu_{C-H}$); 1603, 1553 ($\nu_{C=O}$ and $\nu_{C=N}$); 927s, 902, 896 ($\nu_{Mo=O}$, terminal). **$[MoO_2L(im)]\cdot CH_3CN$.** Solvent used: acetonitrile; red prisms; Elemental analysis

((Calc. (Found) for $C_{17}H_{15}N_5O_5Mo$): C 43.88 (43.82); H 3.25 (3.22); N 15.05 (15.11)). IR (KBr, $cm^{-1}$): 3327m ($\nu_{N-H,\ imidazole}$); 2950, 2843 ($\nu_{C-H}$); 2248 ($\nu_{C\equiv N\ acetonitrile}$); 1600, 1553 ($\nu_{C=O}$ and $\nu_{C=N}$); 924s, 902s ($\nu_{Mo=O}$, terminal).

**Synthesis of $[MoO_2L(pic)]\cdot CH_3CN$ (I(Gp)·$CH_3CN$)**

**Solution synthesis from acetonitrile.** $[MoO_2L]$ (**I**) (15 mg; 0.04 mmol) was diluted in 1.5 mL of heated dry acetonitrile. To such prepared solution equimolar amount of *γ*-picoline was added. Orange-red prisms were filtered off and dried after 3 days standing at the room temperature. Yield: 68%. Analyses (elemental analysis, PXRD, IR) show that the synthesised product is $[MoO_2L(pic)]\cdot CH_3CN$ solvate. Product is stable at the air, even when heated to 40 °C. No product was obtained when the solvent was dichloromethane. Elemental analysis for **$[MoO_2L(pic)]\cdot CH_3CN$:** ((Calc. (Found) for $C_{20}H_{18}N_4O_5Mo$): C 48.99 (48.97); H 3.70 (3.66); N 11.43 (11.40)). IR (KBr, $cm^{-1}$): 2995m, 2832m ($\nu_{C-H}$); 2251($\nu_{C\equiv N\ acetonitrile}$); 1618, 1598, 1551 ($\nu_{C=O}$ and $\nu_{C=N}$); 925s, 903s ($\nu_{Mo=O}$, terminal); 740 ($\nu_{Mo-O}$ and $\nu_{Mo-N}$).

**Synthesis of $[(MoO_2L)_2(bpy)]$ (I(Bp)) and $[(MoO_2L)_2(bpy)]\cdot CH_2Cl_2$ (I(Bp)·$CH_2Cl_2$)**

**Solution synthesis from dichloromethane or acetonitrile.** $[MoO_2L]$ (**I**) (15 mg; 0.04 mmol) was diluted in 1.5 mL of heated dry acetonitrile. To such prepared solution 0.5 ratio of 4,4'-bipyridine was added (0.02 mmol). Orange-red prisms were filtered off and dried after 1 day standing at the room temperature. Yield: 63%. Analyses (elemental analysis, PXRD, IR) show that the synthesised product is $[(MoO_2L)_2(bpy)]$ (**I(Bp)**). When the solvent used was dichloromethane, dark red prisms of the dichloromethane solvate were obtained, $[(MoO_2L)_2(bpy)]\cdot CH_2Cl_2$ (**I(Bp)·$CH_2Cl_2$**). Product is stable at the air, even when heated to 40 °C. Elemental analysis for **$[(MoO_2L)_2(bpy)]\cdot CH_2Cl_2$**. Elemental analysis ((Calc. (Found) for $C_{37}H_{30}N_6O_{10}Mo_2Cl_2$): C 45.28 (45.26); H 3.08 (3.10); N 8.56 (8.62)). IR (KBr, $cm^{-1}$): 3043-2849 ($\nu_{C-H}$); 1605, 1596, 1553 ($\nu_{C=O}$ and $\nu_{C=N}$); 927s, 905 ($\nu_{Mo=O}$, terminal); 749, 729 ($\nu_{Mo-O}$ and $\nu_{Mo-N}$).

**$[(MoO_2L)_2(bpy)]$**. Elemental analysis ((Calc. (Found) for $C_{36}H_{28}N_6O_{10}Mo_2$): C 48.23 (48.26); H 3.15 (3.11); N 9.37 (9.42)). IR (KBr, $cm^{-1}$): 3051-2830 ($\nu_{C-H}$); 1598, 1550 ($\nu_{C=O}$ and $\nu_{C=N}$); 928s, 906 ($\nu_{Mo=O}$, terminal); 744, 733 ($\nu_{Mo-O}$ and $\nu_{Mo-N}$).

# Infrared spectroscopy

In all three alcohol complexes strong doublet at 938 and 914 $cm^{-1}$ is denoted to the symmetric and asymmetric stretching mode of *cis*-$MoO_2^{2+}$ moiety. There can be observed shift in the stretching frequencies characteristic for C=O and C=N of $H_2L$ (from 1617 $cm^{-1}$ and 1577 $cm^{-1}$ in $H_2L$ to 1605 and 1558 $cm^{-1}$ in molybdenum complexes) after the complexation process. This shift is consistent with emergence of coordinated C⋯O and C⋯N groups. Band-patterns in the range of 1620-1200 $cm^{-1}$ are similar for all complexes included in this study, but the sharp band at ~1014 $cm^{-1}$ is characteristic exclusively for enol complexes and is assigned to C–O stretching vibration of coordinated alcohol. Shift in the bands characteristic for O–H group of the alcohol molecule (weakening of the band at ~3400 $cm^{-1}$ and strengthening of the 2500 $cm^{-1}$ band) after the coordination is in agreement with emergence of strong intermolecular O–H⋯N hydrogenbond.

Disappearance of 1014 $cm^{-1}$ band during the heating or grinding of enol complexes is in accordance with surmised dissociation of molybdenum-alcohol coordination bond. Band patterns of **$(I)_n$** and **I** display significant alterations in the 1000-500 $cm^{-1}$ range emphasizing different coordination environment of central molybdenum cation. In **$(I)_n$**, weakening of one $Mo{=}O_{terminal}$ vibration band (915 $cm^{-1}$) and raise of strong and broad band at 818 $cm^{-1}$ refers to vibration of Mo=O⋯Mo moiety. It is well established fact that pentacoordinated molybdenum(VI) complexes aspire to fulfil their coordination sphere by this interaction, yielding polymeric or dimeric structures and that those interaction are clearly visible in the IR spectra.[ii,iii] In **I**, bands pattern is similar to enol complexes (with exception of enol C–O stretching frequency at 1014 $cm^{-1}$). In the spectra there can not be observed bands denoting interaction between the molybdenum centres. This fact suggests that amorphous $[MoO_2L]$ is mononuclear complex with vacant sixth coordination site.

During the syntheses of the octahedral complexes with N-donors, three solvated, $[MoO_2L(im)]\cdot CH_3CN$ (**$I(Im)\cdot CH_3CN$**), $[MoO_2L(pic)]\cdot CH_3CN$ (**$I(Gp)\cdot CH_3CN$**), and $[(MoO_2L)_2(bpy)]\cdot CH_2Cl_2$ (**$I(Bp)\cdot CH_2Cl_2$**), and two products without crystalline solvent were collected, $[MoO_2L(im)]$ (**I(Im)**) and $[(MoO_2L)_2(bpy)]$ (**I(Bp)**). All products display spectra characteristic for mononuclear octahedral molybdenum(VI) complexes, with two strong bands at ~930 and ~905 $cm^{-1}$ emphasising the $\nu_{asym}$ and $\nu_{sym}$ $Mo{=}O_{terminal}$ stretching frequencies. In the spectra of solvated and unsolvated products with the same N-donor, subtle differences can

be observed. Comparing with the data from the diffraction experiments, it is evident that included solvent have significant influence on the molecular and crystal structures. These alterations reflect themselves in the IR patterns. In the spectra of imidazole complexes, **I(im)** and **I(im)·$CH_3CN$**, main difference can be observed in the position of the N–H(imidazole) stretching frequency. In the acetonitrile solvate, same group is involved in the monomeric $C_1^1(9)$ N–H···O5 hydrogen bond, building chain-like structure. In the unsolvated imidazole complex, N–H group of the coordinated imidazole is involved in the symmetric $R_2^2(12)$ N–H···O2 hydrogen bond resulting in the expected shift of the N–H stretching frequency. Since this dimeric hydrogen bond involves terminal Mo=O groups, corresponding band (928 $cm^{-1}$) is seen as doublet. In the acetonitrile solvate, weak but characteristic C≡N stretching frequency can be observed at the ~2251 $cm^{-1}$. In solvent-free synthesis, it represented good qualitative indicator whether the acetonitrile remaines in the structure after the LAG procedure. Same bond can be observed in the **I(Gp)·$CH_3CN$** (2251 $cm^{-1}$). In the spectra of **I(Bp)·$CH_2Cl_2$** and **I(Bp)** no major differences can be observed, except position of the Mo=O stretching frequencies and richer pattern corresponding to C–H vibrations in dichloromethane solvate.

**Grinding of alcohol complexes**

All three alcohol compounds were ground using mortar and pestle, thus allowing evaporation of the dissociated alcohol molecules. In all grinded samples same product was obtained, [$MoO_2L$] (**I**), but the time needed for the liberation of the alcohol molecules was significantly increased together with the ebullition point of coordinated alcohol. Although only two minutes were sufficient for complete transformation in **I(Me)**, more than 35 minutes of vigorous grinding was needed when the *n*-propanol was coordinated (20 minutes for **I(Et)**).

# Thermal experiments

The samples for thermogravimetric measurements were dried in the air and over $CaCl_2$ until the constant mass.

**TGA measurements carried out under oxygen atmosphere.** All alcohol complexes, $[MoO_2(L)(ROH)]$, show similar thermal behaviour. They are stable up to ~90 °C after which they start to decompose in three steps. The first step [94–202 °C; 7.98% **I(Me)**; 80–182 °C; 11.22 **I(Et)**; 90–174 °C; 13.89% **I(Pr)**] is in good agreement with the calculated mass fraction of the coordinated alcohol molecule [7.96 % (**I(Me)**); 11.16 % **I(Et)**; 13.95% **I(Pr)**)]. After the loss of the coordinated solvent molecule intermediate product, $\mathbf{(I)_n}$, is formed and is stable[1] in the temperature range 202–241 °C **I(Me)**); 183–231 °C **I(Et)**); 175–241 °C **I(Pr)**)]. Remaining two steps are assigned to decomposition of organic ligand. In **I** and $\mathbf{(I)_n}$ no mass losses were observed before 210 °C, and deterioration pattern after that temperature is similar to alcohol complexes. Although it was not possible to correlate the weight losses in remaining steps to decomposed organic fragments (oxygen atmosphere), the residues were found to be in good agreement with the formation of $MoO_3$ (PXRD). Thermogravimetric method is known to be suitable for determining of molybdenum mass fraction in dioxomolybdenum-organic coordination compounds. In the case of complexes with N-donors, first thermal event in the solvated species correspond to the solvent molecule egress. Due to the strength of the intermolecular forces stabilizing solvent in the crystalline environment, acetonitrile will leave the $\mathbf{I(Gp)\cdot CH_3CN}$ framework at more than 30 °C higher temperature than in the imidazole solvate, $\mathbf{I(Im)\cdot CH_3CN}$ (Figure S1b and S1c).

[1] $[MoO_2L]_n$ is stable at room temperature for months.

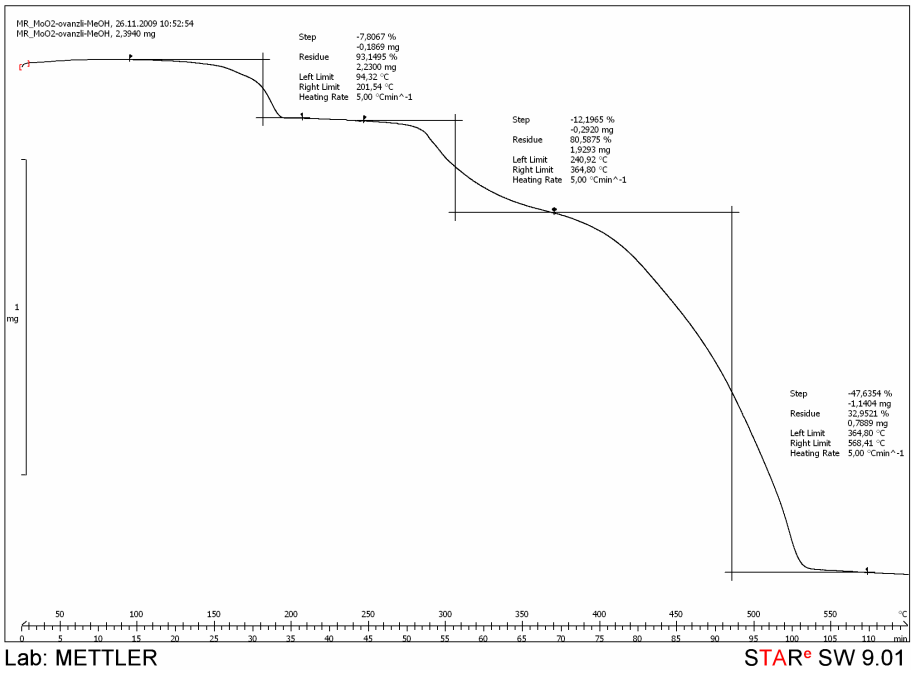
MR_MoO2-ovanzli-MeOH, 26.11.2009 10:52:54
MR_MoO2-ovanzli-MeOH, 2,3940 mg
Step -7,8067 %
-0,1869 mg
Residue 93,1495 %
2,2300 mg
Left Limit 94,32 °C
Right Limit 201,54 °C
Heating Rate 5,00 °Cmin^-1
Step -12,1965 %
-0,2920 mg
Residue 80,5875 %
1,9293 mg
Left Limit 240,92 °C
Right Limit 364,80 °C
Heating Rate 5,00 °Cmin^-1
Step -47,6354 %
-1,1404 mg
Residue 32,9521 %
0,7889 mg
Left Limit 364,80 °C
Right Limit 568,41 °C
Heating Rate 5,00 °Cmin^-1
mg
°C
min
Lab: METTLER
STARe SW 9.01

(a)

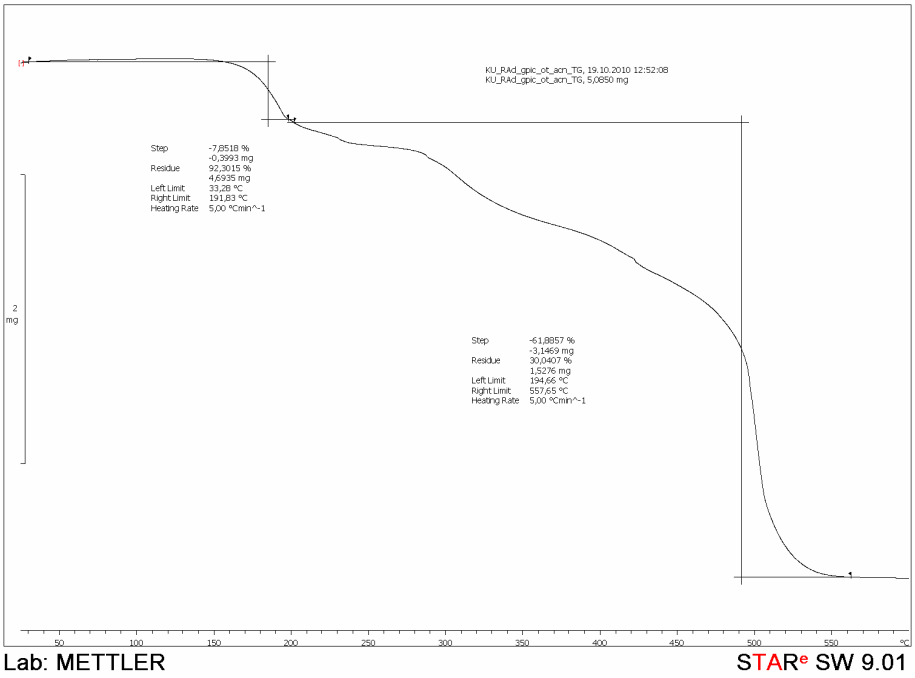
KU_RAd_gpic_ot_acn_TG, 19.10.2010 12:52:08
KU_RAd_gpic_ot_acn_TG, 5,0850 mg
Step -7,8518 %
-0,3993 mg
Residue 92,3015 %
4,6935 mg
Left Limit 33,28 °C
Right Limit 191,83 °C
Heating Rate 5,00 °Cmin^-1
Step -61,8857 %
-3,1469 mg
Residue 30,0407 %
1,5276 mg
Left Limit 194,66 °C
Right Limit 557,65 °C
Heating Rate 5,00 °Cmin^-1
mg
°C
Lab: METTLER
STARe SW 9.01

(b)

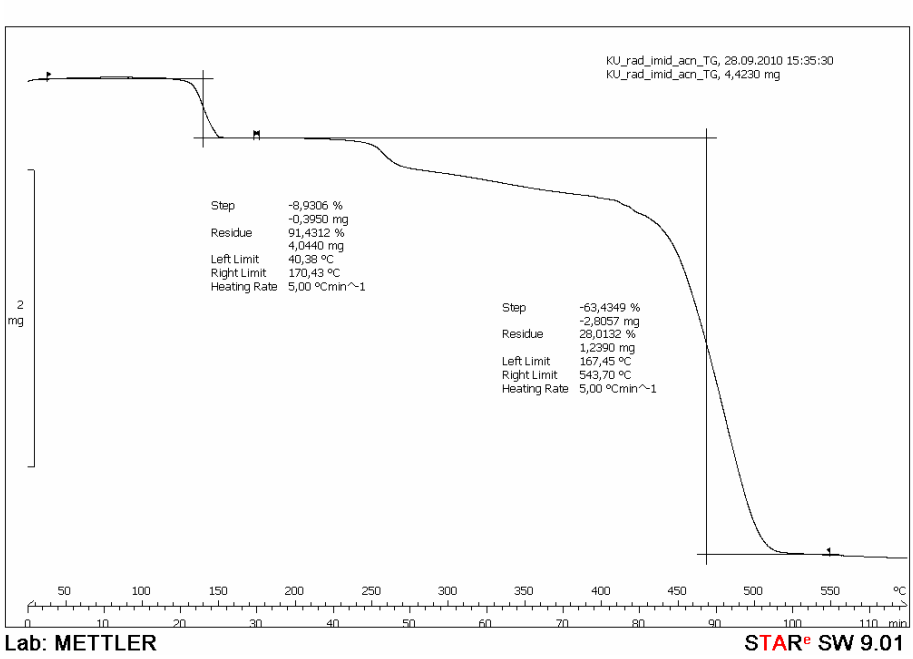
KU_rad_imid_acn_TG, 28.09.2010 15:35:30
KU_rad_imid_acn_TG, 4,4230 mg
Step -8,9306 %
-0,3950 mg
Residue 91,4312 %
4,0440 mg
Left Limit 40,38 °C
Right Limit 170,43 °C
Heating Rate 5,00 °Cmin^-1
Step -63,4349 %
-2,8057 mg
Residue 28,0132 %
1,2390 mg
Left Limit 167,45 °C
Right Limit 543,70 °C
Heating Rate 5,00 °Cmin^-1
2
mg
50 100 150 200 250 300 350 400 450 500 550 °C
0 10 20 30 40 50 60 70 80 90 100 110 min
Lab: METTLER
STARe SW 9.01

(c)

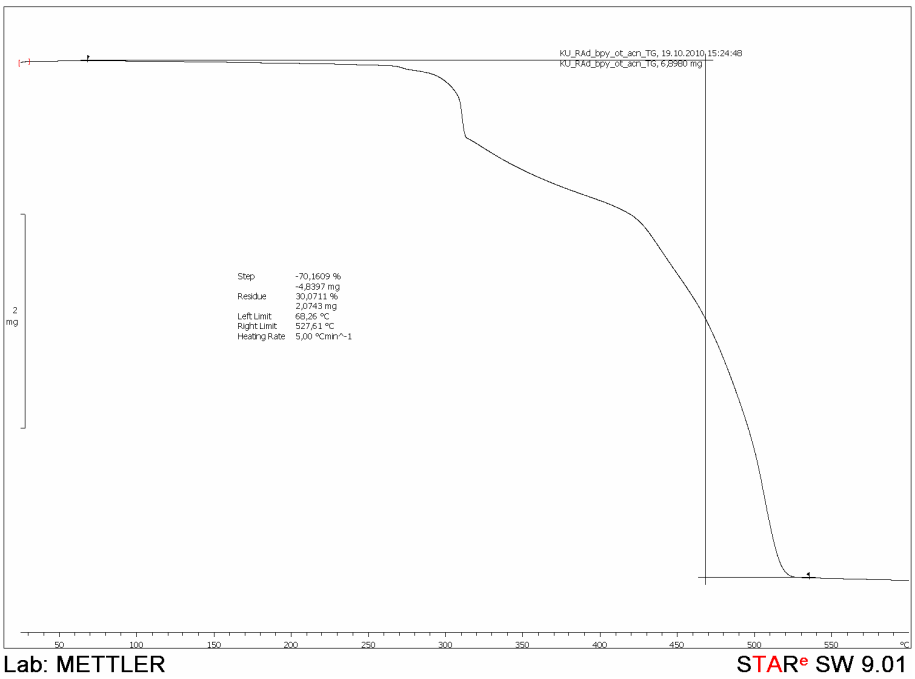
KU_RAd_bpy_ot_acn_TG, 19.10.2010,15:24:48
KU_RAd_bpy_ot_acn_TG, 6,8980 mg
Step -70,1609 %
-4,8397 mg
Residue 30,0711 %
2,0743 mg
Left Limit 68,26 °C
Right Limit 527,61 °C
Heating Rate 5,00 °Cmin^-1
2
mg
50 100 150 200 250 300 350 400 450 500 550 °C
Lab: METTLER
STARe SW 9.01

(d)

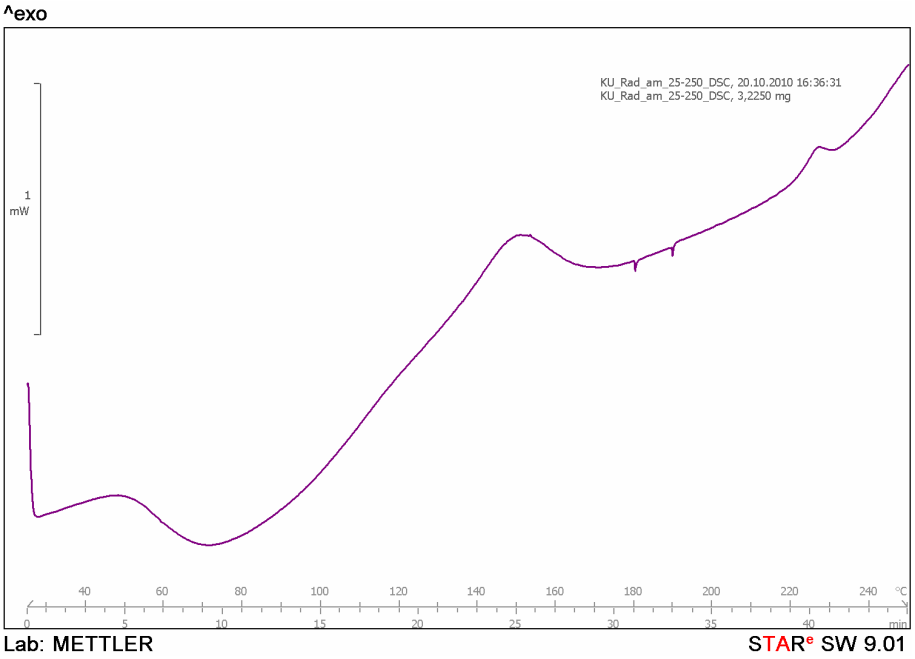


(e)

**Fig. S1.** (a) The TGA curve of **I(Me)**. First thermal event in TGA corresponds to the loss of the methanol molecules. Same deterioration pattern is observed in other alcohol complexes; (b) The TGA curve of **I(Gp)·$CH_3CN$** under oxygen stream. First thermal event is denoted as a loss of crystalline solvent; (c) The TGA curve of **I(Im)·$CH_3CN$** under oxygen stream. First thermal event is denoted as a loss of crystalline solvent; (d) The TGA curve of **I(Bp)** under oxygen stream. Compound is temperature resistant until 250 °C; (e) Broad endotherm and exothermic peak in range of 140-160 °C denotes thermally irreversible phase transition of **I** to **$(I)_n$**.

# X-ray crystallography

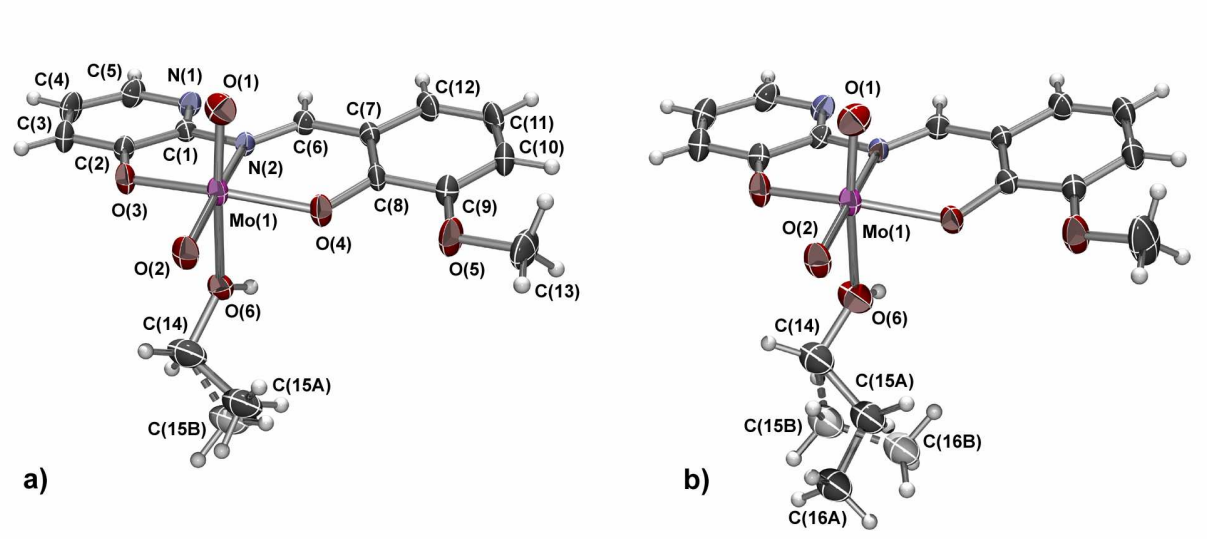


**Fig. S2.** ORTEP-POV-Ray rendered view of the molecular structures for: a) **I(Et)** and b) **I(Pr)** with the atom-numbering schemes. In both structures the ligand atoms are labeled in the same way. The disordered alcohol groups in the positions with lower occupancies are shown in light gray; refined occupancy for the major site of the disordered alcohol group is 0.600(12) in **I(Et)** and 0.598(6) in **I(Pr)**. Displacement ellipsoids are drawn at the 30% probability level. Hydrogen atoms are presented as spheres of arbitrary small radii.

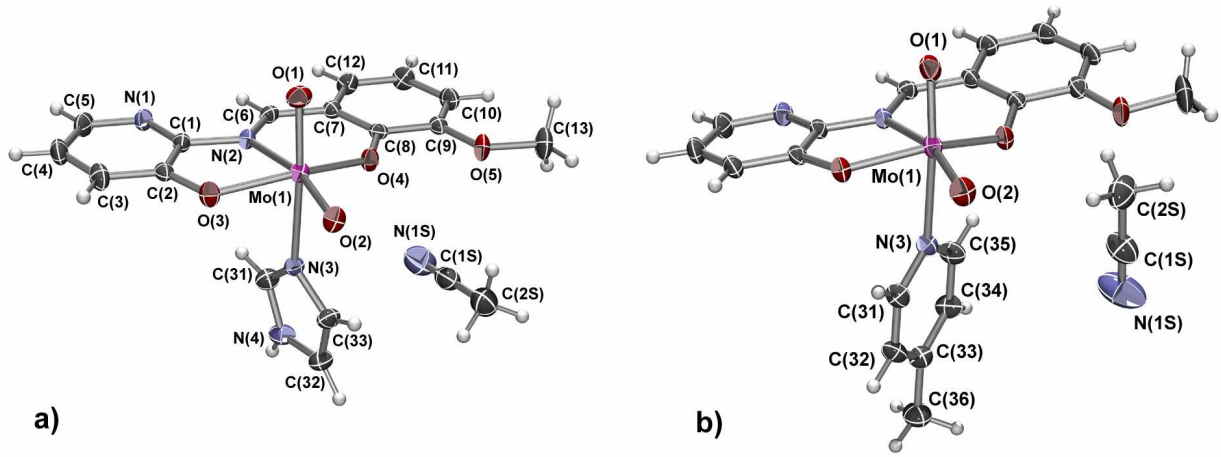


**Fig. S3.** ORTEP-POV-Ray rendered view of the molecular structures for: a) **I(Im)·$CH_3CN$** and b) **I(Gp)·$CH_3CN$** with the atom-numbering schemes. In both structures the ligand atoms are labeled in the same way. Displacement ellipsoids are drawn at the 30% probability level. Hydrogen atoms are presented as spheres of arbitrary small radii.

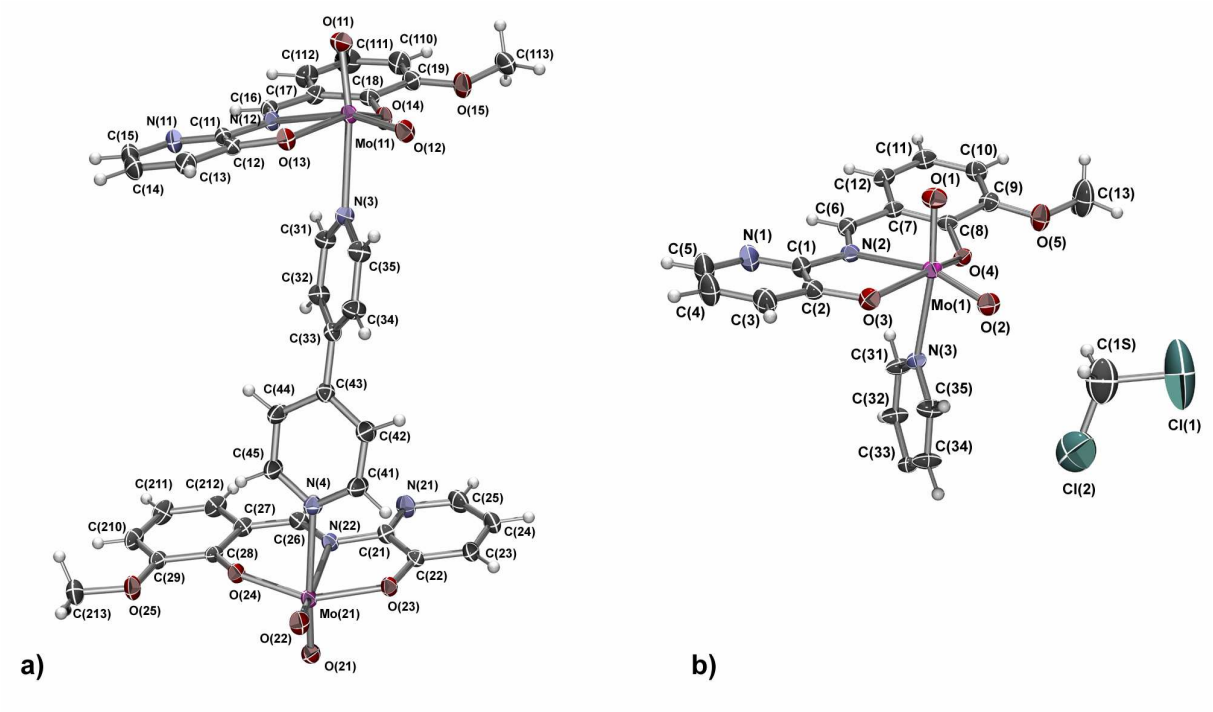


**Fig. S4.** ORTEP-POV-Ray rendered view of the asymmetric units of the: a) **I(Bp)** and b) **I(Bp)·$CH_2Cl_2$** with the atom-numbering schemes. In the **I(Bp)·$CH_2Cl_2$** the other half of the complex is realized through the symmetry operator 1–*x*, –*y*, 2–*z*. Displacement ellipsoids are drawn at the 30% probability level. Hydrogen atoms are presented as spheres of arbitrary small radii.

**Table S1.** Selected geometrical parameters for the alcohol complexes, **I(Me)**, **I(Et)** and **I(Pr)**

| Selected interatomic distances / Å | | | | Selected valence angles / ° | | | |
|---|---|---|---|---|---|---|---|
| | **I(Me)** | **I(Et)** | **I(Pr)** | | **I(Me)** | **I(Et)** | **I(Pr)** |
| Mo(1)–O(1) | 1.6830(2) | 1.681(3) | 1.687(3) | O(1)–Mo(1)–O(2) | 105.71(8) | 105.62(1) | 105.28(16) |
| Mo(1)–O(2) | 1.6988(2) | 1.689(2) | 1.692(3) | O(1)–Mo(1)–O(3) | 98.52(7) | 98.12(1) | 99.23(14) |
| Mo(1)–O(3) | 1.9892(2) | 1.989(2) | 1.978(3) | O(1)–Mo(1)–O(4) | 97.75(8) | 97.96(1) | 96.92(16) |
| Mo(1)–O(4) | 1.9449(2) | 1.935(3) | 1.929(3) | O(1)–Mo(1)–O(6) | 170.62(7) | 169.18(1) | 169.20(15) |
| Mo(1)–O(6) | 2.3297(2) | 2.318(2) | 2.308(4) | O(1)–Mo(1)–N(2) | 91.98(7) | 93.01(1) | 90.19(13) |
| Mo(1)–N(2) | 2.2868(2) | 2.278(2) | 2.294(3) | O(2)–Mo(1)–O(3) | 96.14(7) | 95.90(1) | 96.07(12) |
| O(3)–C(2) | 1.336(3) | 1.339(4) | 1.339(5) | O(2)–Mo(1)–O(4) | 102.91(7) | 102.95(1) | 103.66(12) |
| C(2)–C(1) | 1.421(5) | 1.389(5) | 1.405(5) | O(2)–Mo(1)–O(6) | 83.67(7) | 85.17(1) | 85.44(15) |
| C(1)–N(2) | 1.410(2) | 1.411(4) | 1.402(5) | O(2)–Mo(1)–N(2) | 161.31(7) | 160.24(1) | 163.18(14) |
| N(2)–C(6) | 1.296(2) | 1.279(4) | 1.302(5) | O(3)–Mo(1)–O(4) | 150.50(6) | 150.85(9) | 150.15(12) |
| C(6)–C(7) | 1.427(3) | 1.437(5) | 1.434(6) | O(3)–Mo(1)–O(6) | 80.51(6) | 79.63(9) | 80.64(13) |
| C(7)–C(8) | 1.404(3) | 1.394(5) | 1.434(6) | O(3)–Mo(1)–N(2) | 74.86(6) | 74.61(9) | 74.54(11) |
| C(8)–O(4) | 1.339(3) | 1.338(4) | 1.342(5) | O(4)–Mo(1)–O(6) | 79.46(7) | 80.02(9) | 78.89(14) |
| | | | | O(4)–Mo(1)–N(2) | 80.14(6) | 80.42(9) | 80.49(10) |
| | | | | N(2)–Mo(1)–O(6) | 78.74(6) | 76.18(9) | 79.33(12) |

**Table S2.** Selected geometrical parameters for mononuclear complexes with *N*-donors, **I(Im)**, **I(Im)·$CH_3CN$** and **I(Gp)·$CH_3CN$**

| Selected interatomic distances / Å | | | | Selected valence angles / ° | | | |
|---|---|---|---|---|---|---|---|
| | **1(Im)·$CH_3CN$** | **1(Im)** | **I(Gp) ·$CH_3CN$** | | **1(Im)·$CH_3CN$** | **1(Im)** | **I(Gp) ·$CH_3CN$** |
| Mo(1)–O(1) | 1.694(3) | 1.6946(1) | 1.698(2) | O(1)–Mo(1)–O(2) | 105.01(1) | 104.89(7) | 106.55(1) |
| Mo(1)–O(2) | 1.693(2) | 1.7043(1) | 1.693(2) | O(1)–Mo(1)–O(3) | 97.53(1) | 98.59(6) | 99.06(9) |
| Mo(1)–O(3) | 1.971(3) | 1.9909(1) | 1.9796(19) | O(1)–Mo(1)–O(4) | 96.44(1) | 98.50(6) | 96.96(1) |
| Mo(1)–O(4) | 1.941(2) | 1.9475(1) | 1.938(2) | O(1)–Mo(1)–N(2) | 90.35(1) | 88.16(6) | 90.00(9) |
| Mo(1)–N(2) | 2.275(3) | 2.2736(1) | 2.273(3) | O(1)–Mo(1)–N(3) | 170.44(1) | 170.06(6) | 168.41(9) |
| Mo(1)–N(3) | 2.365(3) | 2.3736(1) | 2.414(3) | O(2)–Mo(1)–O(3) | 97.26(1) | 100.23(6) | 95.61(1) |
| O(3)–C(2) | 1.342(5) | 1.347(2) | 1.355(4) | O(2)–Mo(1)–O(4) | 101.32(1) | 99.89(6) | 102.75(1) |
| C(2)–C(1) | 1.382(5) | 1.398(3) | 1.392(4) | O(2)–Mo(1)–N(3) | 84.52(1) | 85.04(6) | 85.05(1) |
| C(1)–N(2) | 1.428(5) | 1.411(2) | 1.416(4) | O(2)–Mo(1)–N(2) | 163.81(1) | 166.78(6) | 162.28(1) |
| N(2)–C(6) | 1.282(5) | 1.286(2) | 1.288(4) | O(3)–Mo(1)–O(4) | 152.96(1) | 149.19(5) | 151.02(8) |
| C(6)–C(7) | 1.440(6) | 1.441(2) | 1.430(5) | O(3)–Mo(1)–N(3) | 81.66(1) | 79.39(5) | 79.32(9) |
| C(7)–C(8) | 1.395(5) | 1.406(2) | 1.406(5) | O(3)–Mo(1)–N(2) | 75.27(1) | 75.24(5) | 75.09(9) |
| C(8)–O(4) | 1.339(4) | 1.342(2 | 1.344(4) | O(4)–Mo(1)–N(3) | 80.75(11) | 79.36(5) | 80.14(9) |
| | | | | O(4)–Mo(1)–N(2) | 81.61(1) | 79.89(5) | 80.94(9) |
| | | | | N(2)–Mo(1)–N(3) | 80.22(1) | 81.92(5) | 78.48(9) |

**Table S3.** Selected geometrical parameters for the dinuclear complex, **I(Bp)·$CH_2Cl_2$**

| Selected interatomic distances / Å | | Selected valence angles / ° | |
|---|---|---|---|
| | **I(Bp)·$CH_2Cl_2$** | | **I(Bp)·$CH_2Cl_2$** |
| Mo(1)–O(1) | 1.703(3) | O(1)–Mo(1)–O(2) | 106.71(1) |
| Mo(1)–O(2) | 1.698(3) | O(1)–Mo(1)–O(3) | 99.57(1) |
| Mo(1)–O(3) | 1.971(2) | O(1)–Mo(1)–O(4) | 96.94(1) |
| Mo(1)–O(4) | 1.937(2) | O(1)–Mo(1)–N(2) | 90.61(2) |
| Mo(1)–N(2) | 2.277(4) | O(1)–Mo(1)–N(3) | 168.97(1) |
| Mo(1)–N(3) | 2.417(3) | O(2)–Mo(1)–O(3) | 95.69(1) |
| O(3)–C(2) | 1.337(6) | O(2)–Mo(1)–O(4) | 102.44(1) |
| C(2)–C(1) | 1.407(5) | O(2)–Mo(1)–N(2) | 161.72(1) |
| C(1)–N(2) | 1.403(5) | O(2)–Mo(1)–N(3) | 84.14(1) |
| N(2)–C(6) | 1.294(4) | O(3)–Mo(1)–O(4) | 150.78(9) |
| C(6)–C(7) | 1.436(5) | O(3)–Mo(1)–N(2) | 75.25(1) |
| C(7)–C(8) | 1.399(7) | O(3)–Mo(1)–N(3) | 80.92(1) |
| C(8)–O(4) | 1.337(4) | O(4)–Mo(1)–N(2) | 80.65(1) |
| | | O(4)–Mo(1)–N(3) | 78.38(9) |
| | | N(2)–Mo(1)–N(3) | 78.82(1) |

**Table S4.** Selected geometrical parameters for dinuclear **I(Bp)**

| Selected interatomic distances / Å | | Selected valence angles / ° | |
|---|---|---|---|
| | **1(Bp)** | | **1(Bp)** |
| Mo(11)–O(11) | 1.694(3) | O(11)–Mo(11)–O(12) | 106.15(1) |
| Mo(11)–O(12) | 1.697(2) | O(11)–Mo(11)–O(13) | 99.95(1) |
| Mo(11)–O(13) | 1.984(3) | O(11)–Mo(11)–O(14) | 98.63(1) |
| Mo(11)–O(14) | 1.933(3) | O(11)–Mo(11)–N(12) | 91.05(1) |
| Mo(11)–N(12) | 2.288(3) | O(11)–Mo(11)–N(3) | 169.65(1) |
| Mo(11)–N(3) | 2.441(3) | O(12)–Mo(11)–O(13) | 96.80(1) |
| O(13)–C(12) | 1.341(4) | O(12)–Mo(11)–O(14) | 101.98(1) |
| C(12)–C(11) | 1.391(5) | O(12)–Mo(11)–N(12) | 162.07(1) |
| C(11)–N(12) | 1.413(5) | O(12)–Mo(11)–N(3) | 84.13(1) |
| N(12)–C(16) | 1.282(5) | O(13)–Mo(11)–O(14) | 148.66(1) |
| C(16)–C(17) | 1.429(5) | O(13)–Mo(11)–N(12) | 74.78(1) |
| C(17)–C(18) | 1.415(4) | O(13)–Mo(11)–N(3) | 77.20(1) |
| C(18)–O(14) | 1.346(4) | O(14)–Mo(11)–N(12) | 79.88(1) |
| | | O(14)–Mo(11)–N(3) | 80.00(1) |
| | | N(12)–Mo(11)–N(3) | 78.61(1) |
| | | | |
| Mo(12)–O(21) | 1.697(3) | O(21)–Mo(12)–O(22) | 106.65(1) |
| Mo(12)–O(22) | 1.687(3) | O(21)–Mo(12)–O(23) | 98.00(1) |
| Mo(12)–O(23) | 1.981(2) | O(21)–Mo(12)–O(24) | 98.08(1) |
| Mo(12)–O(24) | 1.944(2) | O(21)–Mo(12)–N(22) | 92.24(1) |
| Mo(12)–N(22) | 2.285(4) | O(21)–Mo(12)–N(4) | 167.81(1) |
| Mo(12)–N(4) | 2.469(3) | O(22)–Mo(12)–O(23) | 96.66(1) |
| O(23)–C(22) | 1.345(5) | O(22)–Mo(12)–O(24) | 101.61(1) |
| C(22)–C(21) | 1.394(5) | O(22)–Mo(12)–N(22) | 160.29(1) |
| C(21)–N(22) | 1.421(5) | O(22)–Mo(12)–N(4) | 85.39(1) |
| N(22)–C(26) | 1.292(5) | O(23)–Mo(12)–O(24) | 151.01(1) |
| C(26)–C(27) | 1.423(5) | O(23)–Mo(12)–N(22) | 74.68(1) |
| C(27)–C(28) | 1.418(5) | O(23)–Mo(12)–N(4) | 78.21(1) |
| C(28)–O(24) | 1.345(4) | O(24)–Mo(12)–N(22) | 80.73(1) |
| | | O(24)–Mo(12)–N(4) | 81.02(1) |
| | | N(22)–Mo(12)–N(4) | 75.60(1) |

**Table S5.** C–H···O and C–H··N interactions in the crystal structures of the **I(Me), I(Et)**, **I(Pr)**, **I(Im)**, **I(Im)·$CH_3CN$**, **I(Gp)·$CH_3CN$**, **I(Bp) and I(Bp)·$CH_2Cl_2$**

| C−H···O | *d*(C−H)/Å | *d*(H···O)/Å | *d*(C···O)/Å | ∠(C–H···O)/° | Symmetry operator |
|---|---|---|---|---|---|
| **I(Me)** | | | | | |
| C(4)–H(4)···O(3) | 0.93 | 2.37 | 3.283(3) | 167 | 1–x,1/2+y,1/2–z |
| **I(Et)** | | | | | |
| C(6)–H(6)···O(3) | 0.93 | 2.44 | 3.359(4) | 168 | –x,1/2+y,1/2–z |
| C(15A)–H(15A)···O(5) | 0.96 | 2.56 | 3.375(1) | 143 | –x,1–y,–z |
| **I(Pr)** | | | | | |
| C(11)–H(11)···O(3) | 0.93 | 2.44 | 3.347(6) | 166 | x,-1+y,z |
| C(13)–H(13A)···O(4) | 0.96 | 2.60 | 3.543(6) | 168 | 1-x,-y,1-z |
| C(14)–H(14B)···O(1) | 0.97 | 2.33 | 3.239(6) | 155 | 1+x,y,z |
| C(12)–H(12)···O(1) | 0.93 | 2.49 | 3.218(6) | 136 | 1-x,-y,-z |
| **I(Im)** | | | | | |
| C(4)–H(4)···O(4) | 0.93 | 2.60 | 3.500(3) | 164 | 1–x,1/2+y,3/2–z |
| C(12)–H(12)···O(1) | 0.93 | 2.56 | 3.411(2) | 152 | 1–x,1–y,2–z |
| **I(Im)·$CH_3CN$** | | | | | |
| C(2S)–H(2S2)···O(1) | 0.96 | 2.56 | 3.363(7) | 141 | 1+x,3/2–y,1/2+z |
| C(3)–H(3)···O(2) | 0.93 | 2.46 | 3.218(5) | 138 | x,3/2–y,–1/2+z |
| C(12)–H(12)···O(1) | 0.93 | 2.50 | 3.217(5) | 134 | –x,2–y,–z |
| C(13)–H(13A)···O(2) | 0.96 | 2.49 | 3.418(5) | 162 | x,3/2–y,1/2+z |
| C(31)–H(31)···N(1) | 0.93 | 2.62 | 3.409(5) | 143 | 1–x,2–y,–z |
| C(32)–H(32)···O(3) | 0.93 | 2.46 | 3.352(5) | 161 | 1+x,3/2–y,1/2+z |
| **I(Gp)·$CH_3CN$** | | | | | |
| C(2S)–H(2S3)···O(5) | 0.96 | 2.42 | 3.214(5) | 139 | |
| C(12)–H(12)···O(1) | 0.93 | 2.59 | 3.393(4) | 145 | –x,2–y,–z |
| C(34)–H(34)···O(1) | 0.93 | 2.52 | 3.435(5) | 167 | –x,1/2+y,1/2–z |
| **I(Bp)** | | | | | |
| C(14)–H(14)···O(21) | 0.93 | 2.57 | 3.145(5) | 121 | –1+x,–1+y,–1+z |
| C(34)–H(34)···O(25) | 0.93 | 2.33 | 3.210(6) | 158 | 1-x,1-y,1-z |
| C(111)–H(111)···O(23) | 0.93 | 2.42 | 3.321(5) | 163 | x,-1+y,-1+z |
| C(112)–H(112)···O(22) | 0.93 | 2.47 | 3.291(5) | 148 | x,-1+y,-1+z |
| C(210)–H(210)···O(21) | 0.93 | 2.45 | 3.157(5) | 133 | 2-x,2-y,1-z |
| C(211)–H(211)···O(13) | 0.93 | 2.57 | 3.470(5) | 162 | 1+x,1+y,z |

| **I(Bp)·$CH_2Cl_2$** | | | | | |
|---|---|---|---|---|---|
| C(1S)–H(1)···N(1) | 0.97 | 2.48 | 3.411(7) | 162 | 1-x,1/2+y,3/2-z |
| C(1S)–H(2)···O(2) | 0.97 | 2.59 | 3.397(9) | 140 | |
| C(32)–H(32)···O(1) | 0.93 | 2.48 | 3.407(4) | 172 | 1-x,-1/2+y,3/2-z |
| C(34)–H(34)···O(1) | 0.93 | 2.42 | 3.345(6) | 174 | x,1/2-y,1/2+z |

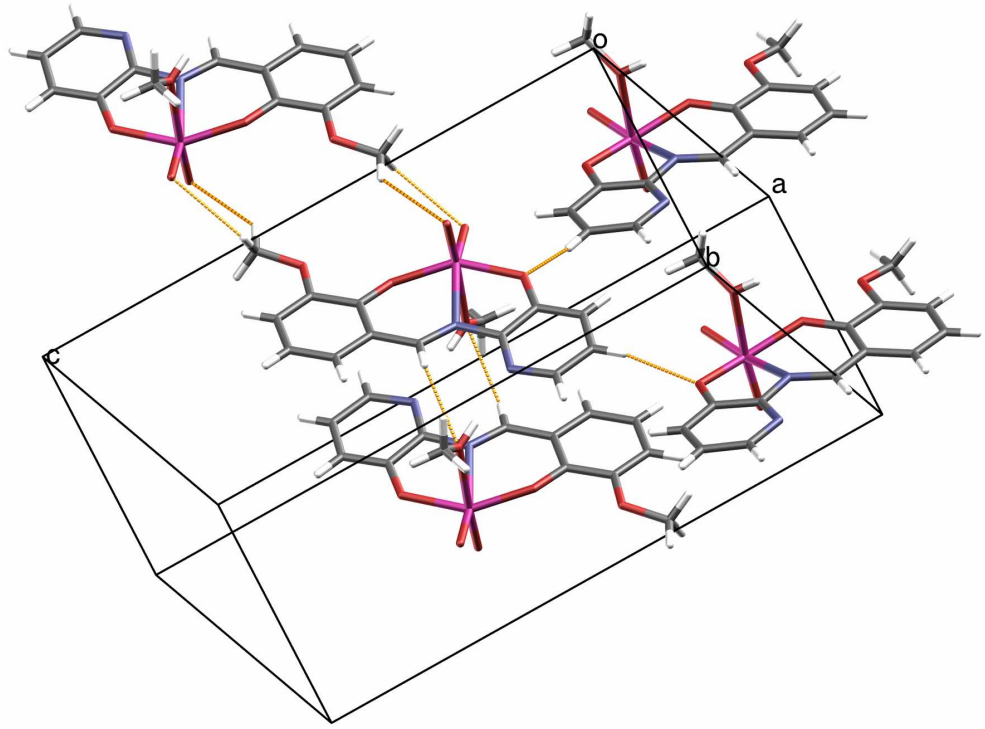


**Fig. S5.** The packing diagram of **I(Me)** viewed almost down the *a* axis showing C–H···O interactions (yellow dashed lines) building complex three-dimensional network.

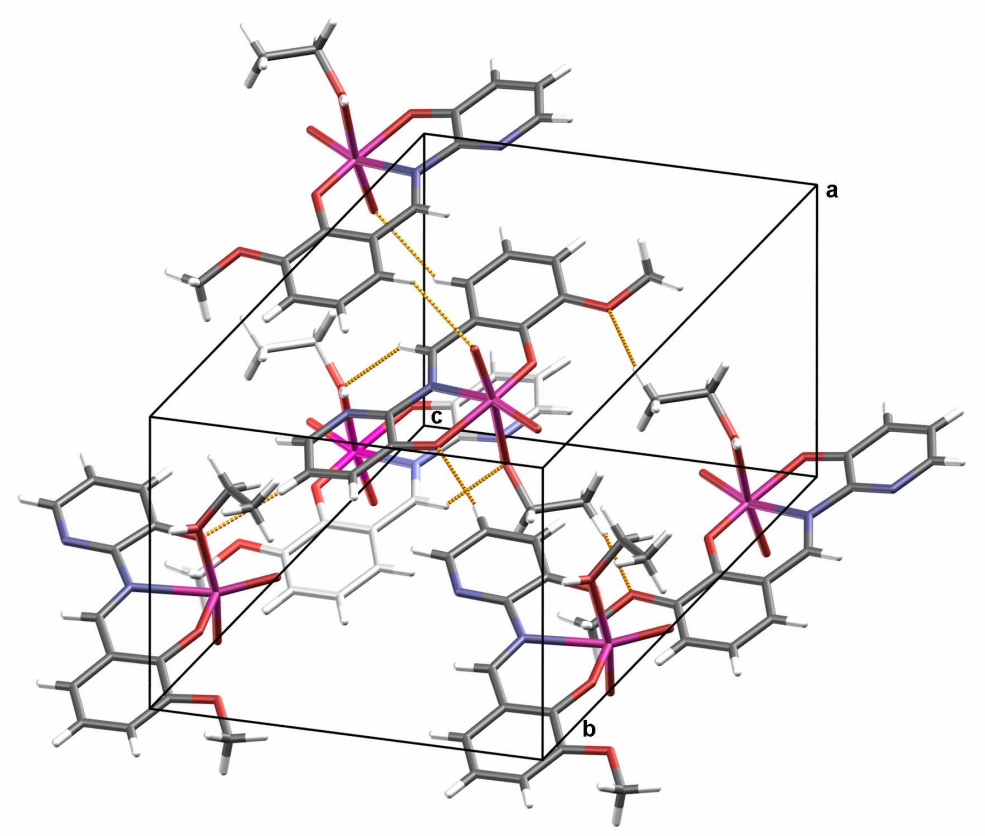


**Fig. S6.** The packing diagram of **I(Et)** showing C–H···O interactions (yellow dashed lines).

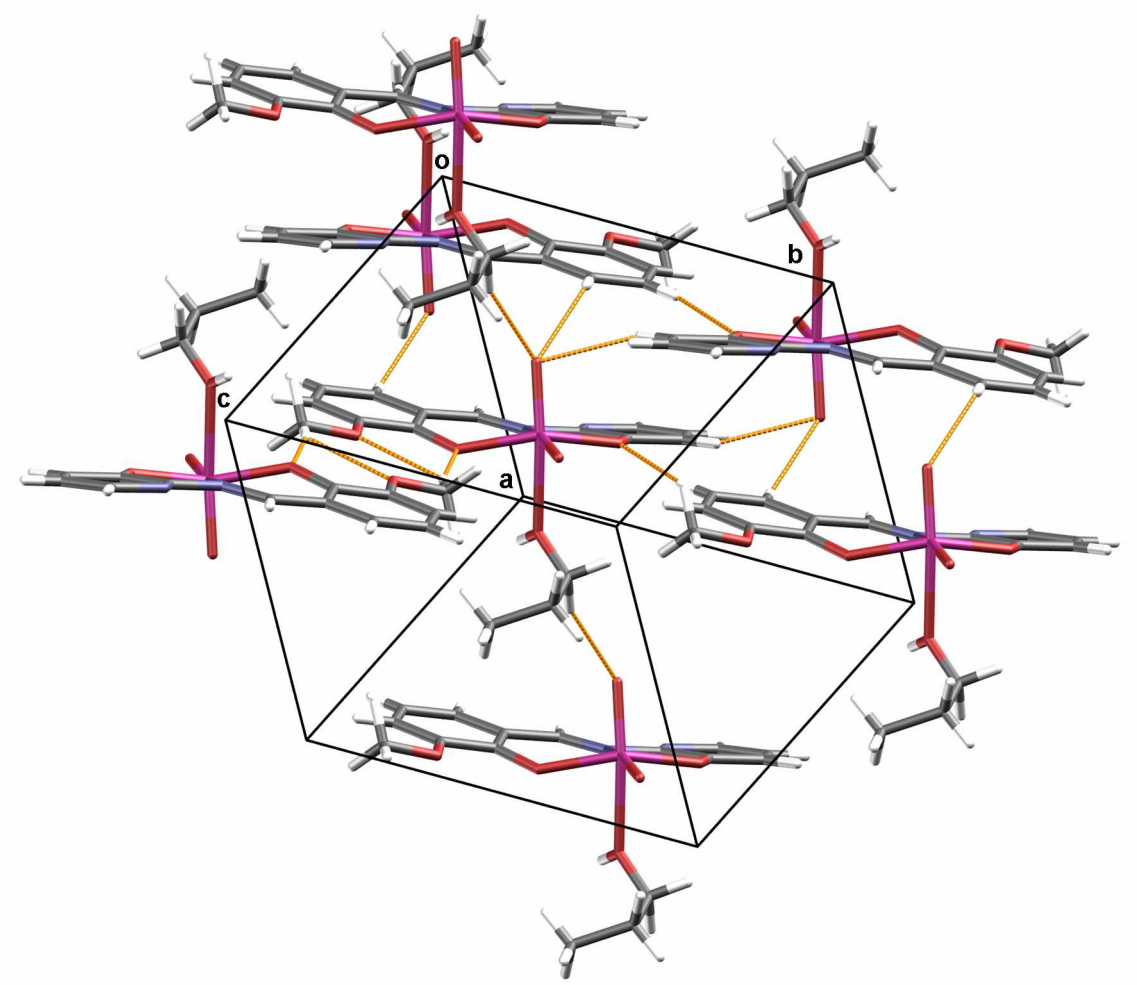


**Fig. S7.** The packing diagram of **I(Pr)** showing C–H···O interactions (yellow dashed lines).

.

.

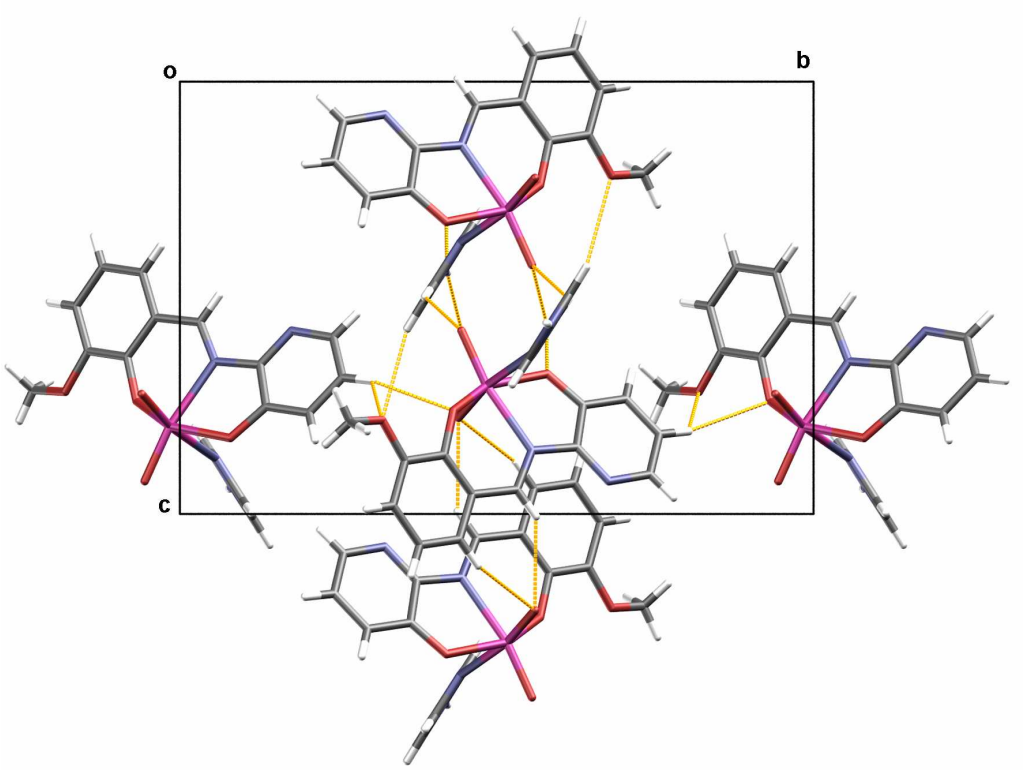


**Fig. S8.** The packing diagram of **I(Im)** viewed down the *a* axis showing C–H···O interactions (yellow dashed lines) building complex three-dimensional network.

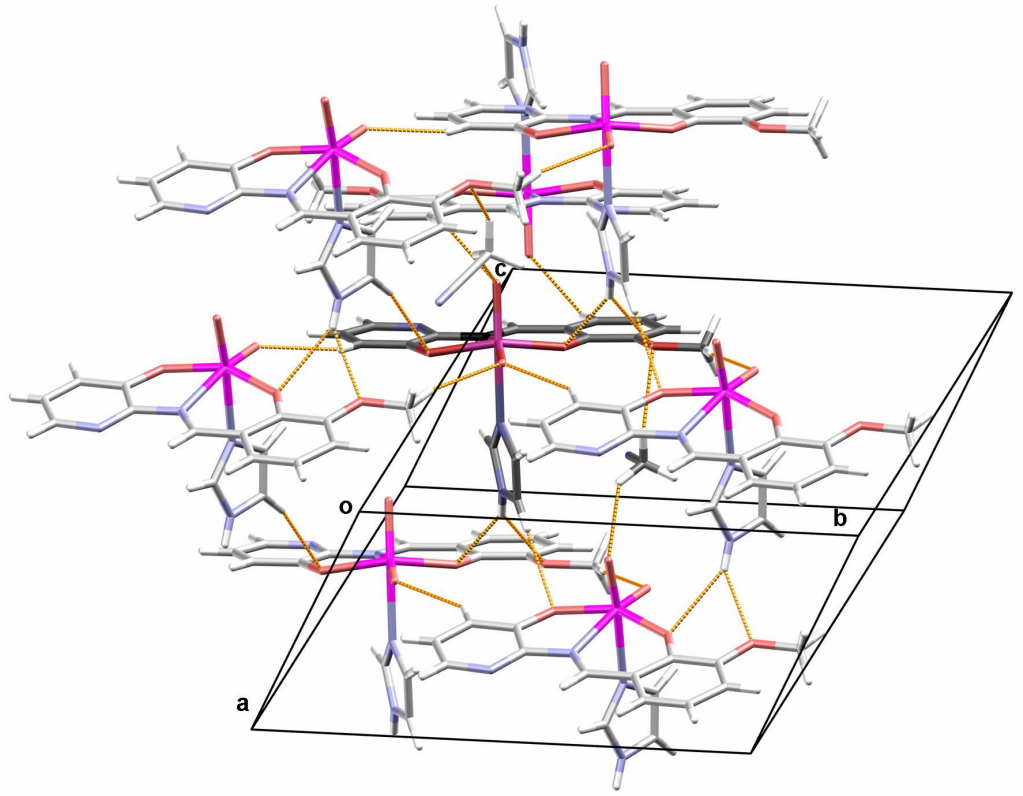


**Fig. S9.** The packing diagram of **I(Im)·$CH_3CN$** showing N–H···O hydrogen bonds and C–H···O interactions (yellow dashed lines) building complex three-dimensional network.

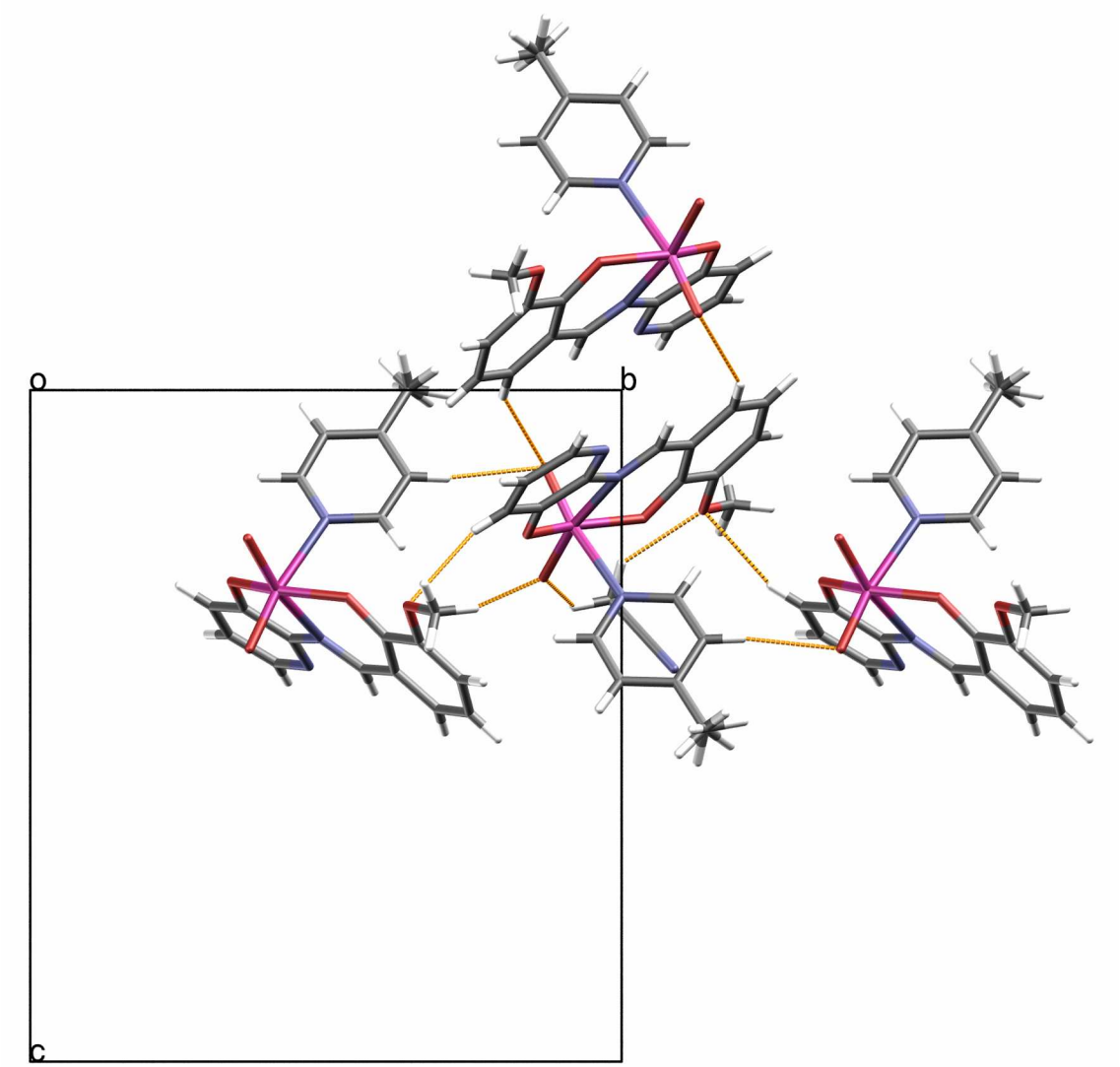


**Fig. S10.** The packing diagram of **I(Gp)·$CH_3CN$** viewed down the *a* axis showing C–H···O interactions (yellow dashed lines).

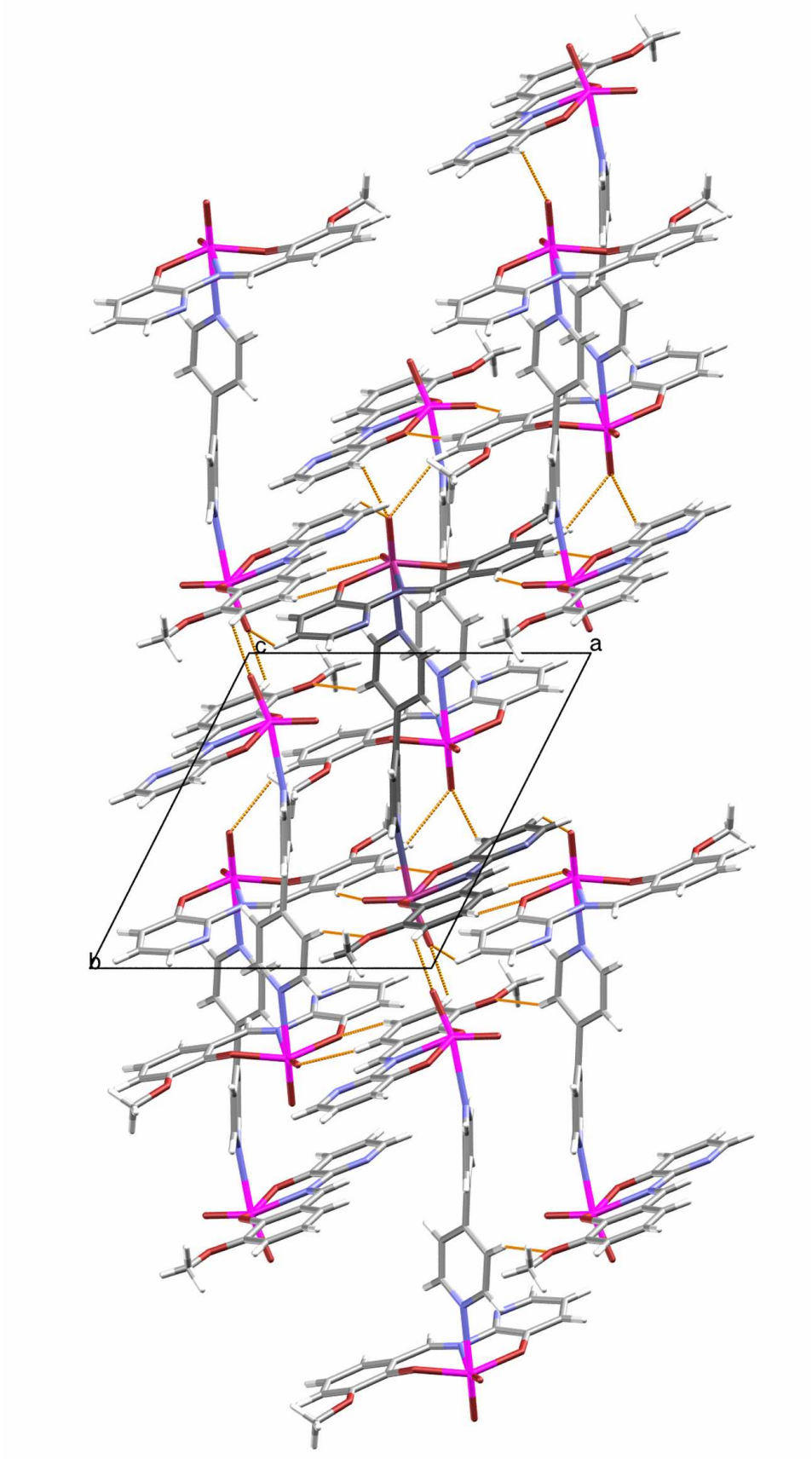


**Fig. S11.** The packing diagram of **I(Bp)** viewed down the *c* axis showing C–H···O interactions (yellow dashed lines).

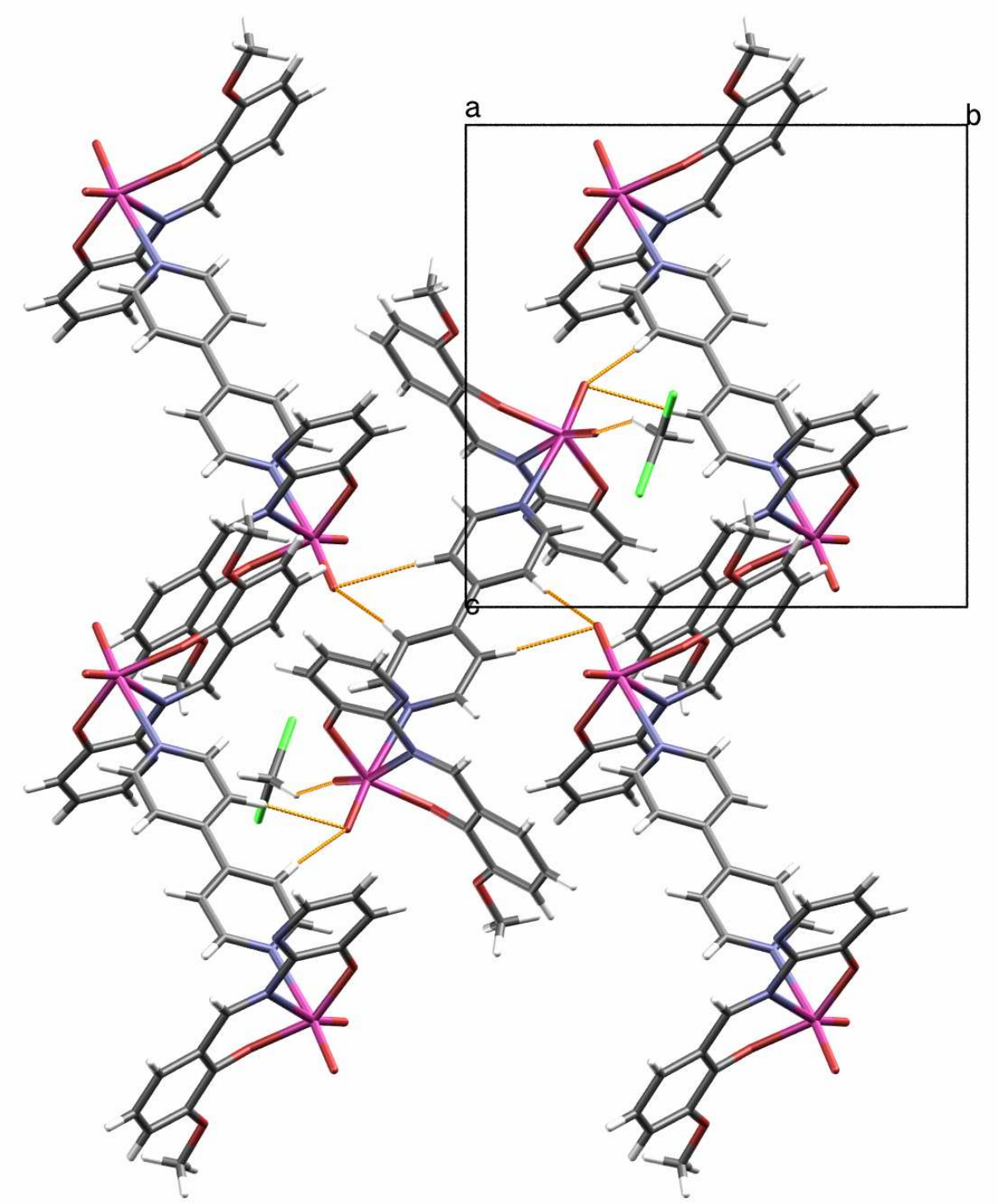


**Fig. S12.** The packing diagram of **I(Bp)·$CH_2Cl$** viewed down the *a* axis showing C–H···O interactions (yellow dashed lines).

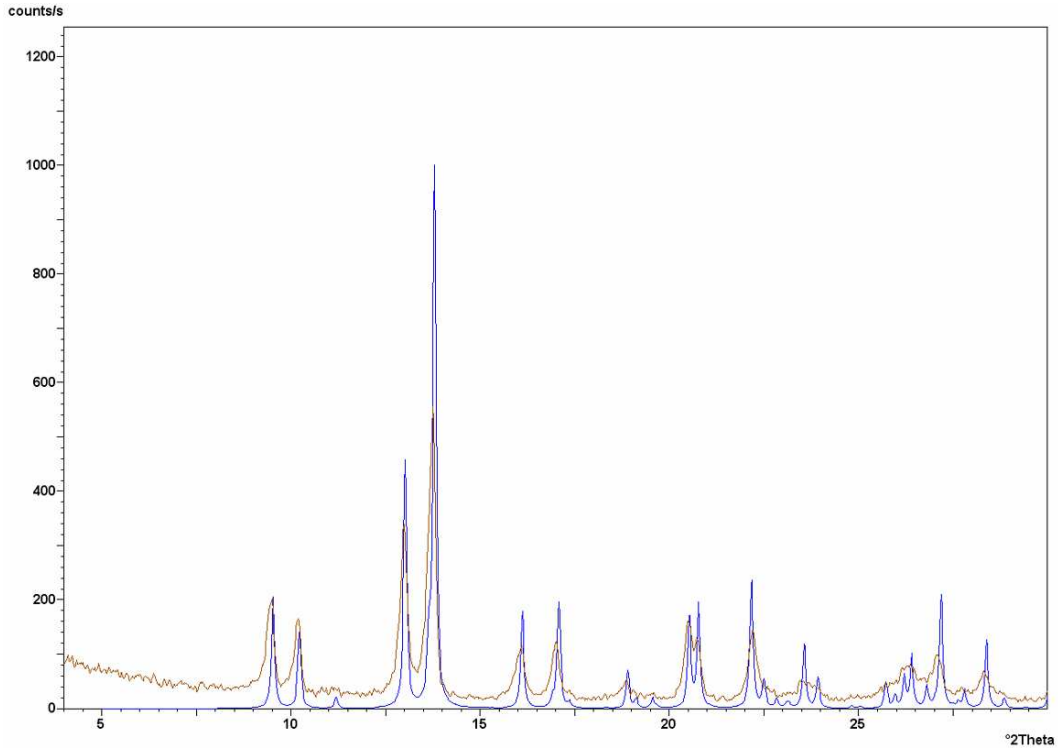


**Fig. S13.** Comparison of PXRD patterns of $[MoO_2L]_n$ (**$(I)_n$**) after methanol vapour sorption (brown) with calculated pattern for $[MoO_2L(MeOH)]$ (**I(Me)**) (blue).

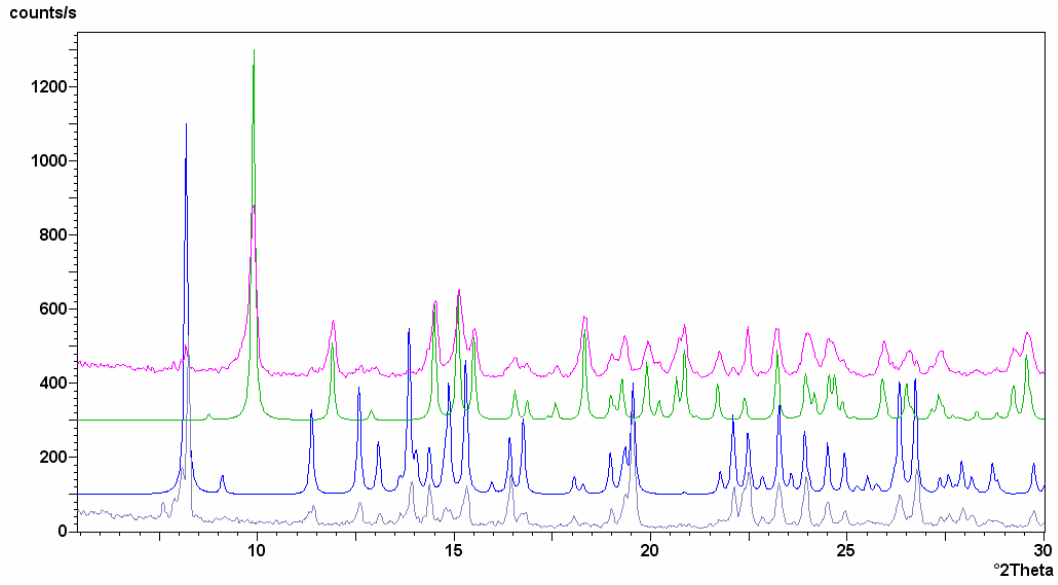


(a)

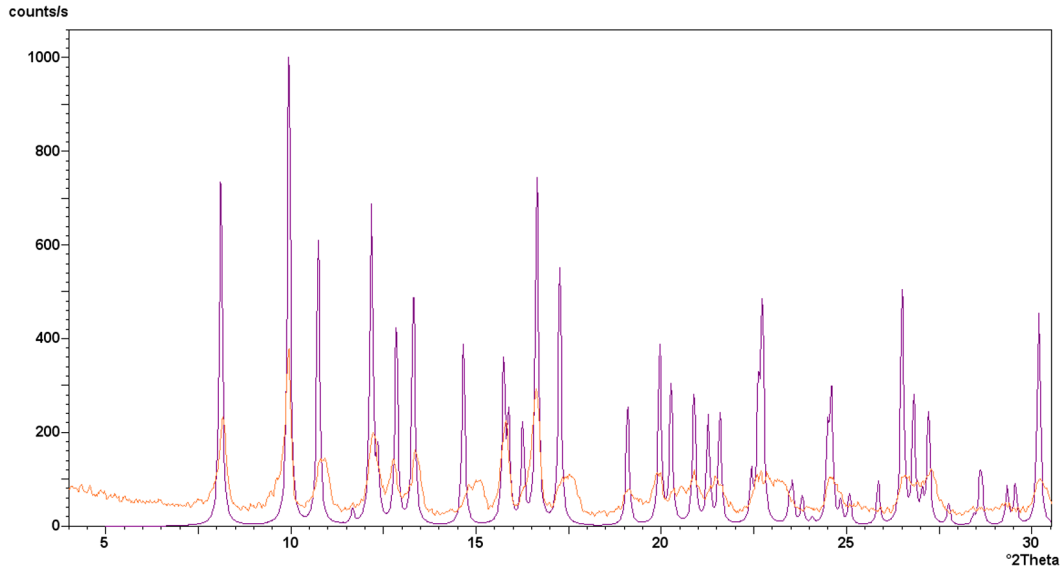


(b)

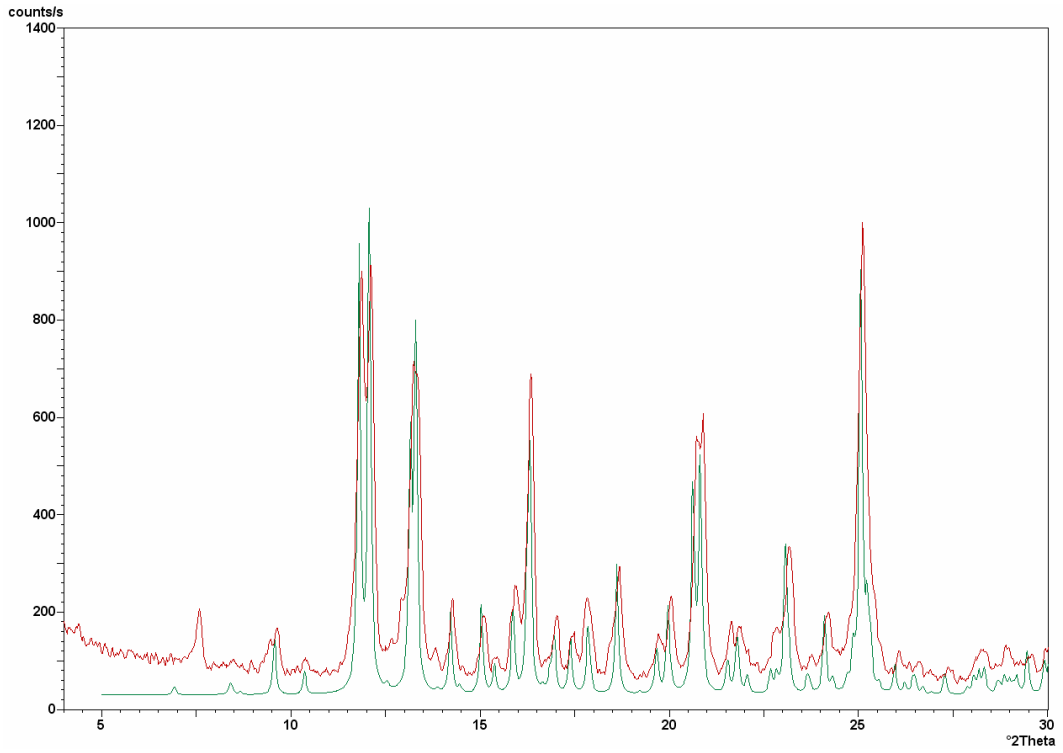


(c)

**Fig. S14.** Comparison of PXRD patterns of products obtained by LAG grinding (40 minutes, 3 drops of solvent) of $[MoO_2L]_n$ and corresponding *N*-donor with calculated patterns from single crystal experiments (a) gray- dichloromethane LAG with imidazole, blue – calculated $[MoO_2L(im)]$; green- acetonitrile LAG, purple calculated $[MoO_2L(im)]\cdot CH_3CN$; (b) orange -

acetonitrile LAG with $\gamma$-picoline, purple calculated $[MoO_2L(pic)]\cdot CH_3CN$; c) red - acetonitrile LAG with 4,4'-bipyridine, green- calculated $[MoO_2L(bpy)]$.

---

[i] G. J.–J. Chen, J. W. McDonald, and W. E. Newton, Inorg. Chem. 1976, **15**, 2612.

[ii] C. G. Young, Molybdenum. In *Comprehensive Coordination Chemistry*, McCleverty, A. J.; Meyer, T. J., Eds.; Pergamon: Oxford, 2004; Chapter 4.7, pp 415–527.

[iii] (a) I. Ivanović, K. Andjelković, V. M. Leovac, Lj. Klisarov, M. Lazarević, and D. Minić, *J. Thermal Anal.* 1996, **46**, 1741. (b) M. Cindrić, N. Strukan, V. Vrdoljak, T. Kajfež and B. Kamenar, *Z. Anorg. Allg. Chem.* 2002, **628**, 2113. (c) O. A. Rajan and A. Chakravorty, *Inorg. Chem.* 1981, **20**, 660.